RC 22065 (98988) 21 May 2001
Materials Science

IBM Research Report

Scanning X-Ray Microtopographs of Misfit Dislocations at SiGe/Si Interfaces

P. M. Mooney, J. L. Jordan-Sweet, S. Christiansen
IBM Research Division
Thomas J. Watson Research Center
P.O. Box 218
Yorktown Heights, NY 10598

Research Division
Almaden - Austin - Beijing - Haifa - T. J. Watson - Tokyo - Zurich

LIMITED DISTRIBUTION NOTICE: This report has been submitted for publication outside of IBM and will probably be copyrighted if accepted for publication. It has been issued as a Research Report for early dissemination of its contents. In view of the transfer of copyright to the outside publisher, its distribution outside of IBM prior to publication should be limited to peer communications and specific requests. After outside publication, requests should be filled only by reprints or legally obtained copies of the article (e.g. payment of royalties). Copies may be requested from IBM T. J. Watson Research Center , P. O. Box 218, Yorktown Heights, NY 10598 USA (email: reports@us.ibm.com). Some reports are available on the internet at http://domino.watson.ibm.com/library/CyberDig.nsf/home

Scanning X-Ray Microtopographs of Misfit Dislocations at SiGe/Si Interfaces

P.M. Mooney, J.L. Jordan-Sweet and S. Christiansen

IBM Research Division

T.J. Watson Research Center

Yorktown Heights, NY 10598

Abstract

Misfit dislocations at $Si_{1-x}Ge_x$/Si interfaces have been imaged by x-ray microdiffraction using the 004 diffraction peak of both the $Si_{1-x}Ge_x$ layer and the Si(001) substrate. At the $Si_{1-x}Ge_x$ layer peak, a decrease in the diffracted intensity is found at dislocations, with features as narrow as 4 microns. Similar features are seen using the Si peak; however, they are usually broader and the diffracted intensity is found to increase at the dislocations. The increased intensity of the Si peak is due to the loss of extinction resulting from the distortion of the crystal lattice near the dislocation. However, the epitaxially-grown $Si_{1-x}Ge_x$ layer is much thinner than the extinction depth; therefore, the distortion of the lattice in the $Si_{1-x}Ge_x$ layer results primarily in the broadening of the $Si_{1-x}Ge_x$ rocking curve with a corresponding decrease in the peak intensity. We also show that the distortion of the crystal lattice extends throughout the entire epitaxial layer structure.

$Si_{1-x}Ge_x$/Si heterostructures are used to fabricate high-speed transistors that extend the range of applications of Si technology. For example, SiGe heterojunction bipolar transistors are used in integrated circuits for analog and mixed-signal applications [1,2]. SiGe field-effect transistors (FETs), in which the active device layers are strained Si or $Si_{1-y}Ge_y$ grown epitaxially on a strain-relaxed $Si_{1-x}Ge_x$ buffer layer, are also under investigation for applications in high-speed digital and analog circuits [2-7].

X-ray microdiffraction has recently been applied to semiconductor heterostructures, for example, to study selective area epitaxial growth of InGaAsP multilayers for optoelectronic devices [8] and to investigate the microstructure of strain-relaxed $Si_{1-x}Ge_x$ buffer layers that are used as virtual substrates for SiGe FETs [9,10]. The latter experiments revealed the presence of local tilted regions having tilt angles that vary by as much as 0.25^o in $Si_{0.83}Ge_{0.17}$ and $Si_{0.69}Ge_{0.31}$ films that are nearly fully relaxed. The local tilted regions, which all have essentially the same lattice parameter and are less than 20 μm in size, result from the network of 60° misfit dislocations that relieve the lattice mismatch strain. Scanning microtopographs taken at the 004 Bragg peak of the relaxed $Si_{1-x}Ge_x$ layer reveal the cross hatch pattern of the misfit dislocations lying along two perpendicular <110> directions due to orientation contrast [11] from the local tilted regions.

Here we report the results of x-ray microdiffraction experiments in $Si_{1-x}Ge_x$ structures where negligible strain relaxation has occurred, i.e., in samples that have a low density of misfit dislocations at the $Si_{1-x}Ge_x$/Si interface. Scanning microtopographs

clearly reveal the inhomogeneous distribution of misfit dislocations in these samples. The mechanisms that give rise to opposite intensity contrast in scanning microtopographs taken at the 004 Bragg peaks of the Si(001) substrate and the $Si_{1-x}Ge_x$ layer are discussed. We also show that the distortion of the crystal lattice by the misfit dislocations extends throughout the entire epitaxial structure.

Structures consisting of either a uniform composition (sample A) or step-graded composition (samples B and C) $Si_{1-x}Ge_x$ layer on a Si(001) substrate were grown by ultra-high vacuum chemical vapor deposition (UHV/CVD) [12]. The alloy composition and degree of strain relaxation of the $Si_{1-x}Ge_x$ layers were determined from high-resolution 004 and 224 x-ray rocking curves taken with a standard laboratory diffractometer. All the SiGe layers were found to be pseudomorphic within the uncertainty of the x-ray measurements. The layer thickness of the uniform composition sample (A) was determined from the Pendell□sung fringes on the x-ray rocking curve. The thickness of each step in the step-graded samples (C and D) was determined from cross-sectional transmission electron microscopy (XTEM) images. The layer characteristics are given in Table I.

Planar view transmission electron micrographs (PVTEM) of these samples show 60° misfit dislocations running along the <110> axes at or near the $Si_{1-x}Ge_x$/Si interface in some areas while other areas are dislocation free. The dislocations occur primarily in pileups [4] rather than as isolated single dislocations. This indicates that dislocation nucleation takes place by a multiplication mechanism, as expected from previous work

[4]. Although details of the multiplication mechanism remain controversial, the inhomogeneous distribution of dislocations in these samples is unambiguous. Atomic force micrographs (AFM), taken over a larger area than the PVTEM images, show the surface steps corresponding to the misfit dislocations and further demonstrate the inhomogeneous distribution of misfit dislocations.

X-ray microdiffraction measurements were performed at beamline X20 at the National Synchrotron Light Source at Brookhaven National Laboratory using IBM's monochromatic microdiffraction system [13,14]. The monochromatic x-ray beam at wavelengths close to Cu $K_{\alpha 1}$ is focused using a 60 μm-diameter capillary tapered down to 2-10 μm, depending on the particular capillary. The focused beam has a divergence of about 0.3^{o} and therefore in the diffraction (vertical) direction only a small fraction of the incident beam, specifically the center of the fan where the intensity is a maximum, is at the proper angle for Bragg diffraction from our single crystal samples [14]. Thus, for a bare Si wafer, the width of the 004 diffracted beam (along the diffraction direction) at the sample is less than 20% of the diameter of the illuminated spot, about 0.2-2 μm, depending on the capillary. For most measurements, the receiving slits in the diffraction direction (vertical) were set to receive the width of the diffracted beam from the bare Si wafer. In the non-diffracting direction (horizontal), the receiving slits were set to accept 2-5 μm of the diffracted beam. The Huber two-circle diffractometer is equipped with partial chi and phi arcs for alignment of our single crystal samples and the x-y stage allows samples to be moved under the beam in steps as small as 1 μm.

To image the misfit dislocations, topographs were taken by scanning the sample, positioned at the symmetric 004 Bragg peak of either the Si substrate or $Si_{1-x}Ge_x$ layer, at constant incident angle under the x-ray beam. Fig. 1 shows a scanning microtopograph taken at the 004 peak of the $Si_{1-x}Ge_x$ layer of sample A. The sample was oriented so that the x and y scanning directions are $\simeq 45^o$ with respect to the <110> crystal axes. Note the pattern of dark lines running parallel to the <110> crystal axes. The variations in the width, 4-12 μm, and the intensity of the dark lines suggest that they originate from pileups of dislocations, rather than single 60° misfit dislocations. The darker and/or wider the line, the more dislocations are present. This interpretation is consistent with the PVTEM images of the dislocated regions of the samples, such as that shown in Fig. 2, and with AFM images such as that shown in Fig. 3. The width of the narrowest lines in the scanning microtopograph is somewhat smaller than the line width of 7 μm reported on topographs of $Si_{1-x}Ge_x$ layers made using a standard high-resolution laboratory x-ray source [15].

The magnitude of the intensity variations was investigated by taking line scans, i.e. scans of the intensity at constant incident angle vs. the x position of the sample at a fixed y position, at the Bragg peaks of both the $Si_{1-x}Ge_x$ layer and the Si substrate. For these measurements, the sample was oriented so as to scan parallel to a <110> crystal axis, i.e. perpendicular (or parallel) to the misfit dislocation lines. As is shown in Fig. 4, similar features are observed in both line scans. However, the dislocations reduce the intensity of the diffracted beam from the $Si_{1-x}Ge_x$ layer while their presence increases the intensity of the diffracted beam from the Si substrate. In this pair of scans, the features in

the scan taken at the Si peak appear to be only slightly broader than those in scans taken at the $Si_{1-x}Ge_x$ layer peak. In some cases, the features taken at the $Si_{1-x}Ge_x$ peak were significantly narrower than those taken at the Si substrate peak.

A similar difference in the intensity contrast on topographs taken using a standard laboratory x-ray beam at the $Si_{1-x}Ge_x$ layer and Si substrate peaks has been reported by Fewster [15]. The contrast difference was explained in terms of the x-ray beam divergence which was greater than the natural width of the Si substrate peak but smaller than the width of the $Si_{1-x}Ge_x$ peak in that case. This explanation cannot be valid in our case, however, since the divergence of the incident microbeam is significantly greater than the natural width of both the Si and $Si_{1-x}Ge_x$ peaks. For the Si substrate peak, the dominant effect is the loss of extinction [11], i.e. kinematic rather than dynamic scattering occurs due to the lattice distortion near the dislocation, thus giving increased diffracted intensity. However, this effect is insignificant when the $Si_{1-x}Ge_x$ layer peak is scanned, since the $Si_{1-x}Ge_x$ layer thickness is $<10\%$ of the extinction depth in Si [16]. Orientation contrast does not apply in this case, since the mosaic broadening of the rocking curves of these strained samples is negligible compared to the divergence of the incident microbeam.

To investigate the contrast mechanism for the $Si_{1-x}Ge_x$ layer, regions of the samples having distinct isolated features in the line scan indicting the presence of relatively few misfit dislocations were explored. Rocking curves (scans of intensity vs. theta, where theta is the angle between the sample surface and the incident beam) were

taken at each point along a line scan, such as the one from sample B shown in Fig. 5(a). Note the features labeled 1 and 2 where the diffracted intensity decreases. Since the change in the peak angle is small compared to the beam divergence, a plot of the rocking curve peak intensity as a function of the position on the sample looks identical to this line scan. The integrated intensity and the full width at half maximum (FWHM) of the rocking curves are also plotted in Fig. 5. The integrated intensity of the rocking curves is essentially constant (Fig. 5(b)) and the decreases in peak intensity, 14% and 29% at positions 1 and 2 respectively, correspond to increases, 13% and 26% respectively, in the FWHM (Fig. 5(c)). The intensity contrast seen in the scanning microtopograph of Fig. 1 is therefore primarily due to the broadening of the rocking curve by the strain field of the dislocations. We also note that the center of the FWHM (Fig. 5(d)) is slightly rotated toward higher theta at positions 1 and 2 indicating a tilting of the crystal lattice by the dislocations as expected. These results suggest that there are twice as many dislocations at position 2 as at position 1.

Finally, in Fig. 6 we show a plot of the line scans taken at the 004 Bragg peaks of the two $Si_{1-x}Ge_x$ layers in sample C. Note that the same intensity variations appear in both scans, clearly demonstrating that the distortion of the crystal lattice by dislocations located near the $Si_{1-x}Ge_x$/Si interface extends throughout both epitaxial layers. This result is consistent with other experiments demonstrating that the surface of a Si or $Si_{1-x}Ge_x$ layer is perturbed by the strain field of a buried dislocation [17,18].

In summary, x-ray microdiffraction images reveal the inhomogeneous distribution of misfit dislocations at $Si_{1-x}Ge_x$/Si interfaces. By recording x-ray rocking curves at various points on the image, we have explored the different contrast mechanisms acting when the image is taken at the Si substrate or $Si_{1-x}Ge_x$ layer diffraction peak. By taking data at different $Si_{1-x}Ge_x$ peaks in the same sample we have shown that the distortion of the crystal lattice extends throughout the entire epitaxial $Si_{1-x}Ge_x$ layer structure.

We acknowledge J.O. Chu for epitaxial growth of the $Si_{1-x}Ge_x$ samples, F.K. LeGoues for cross sectional TEM measurements, and S.K. Kaldor and I.C. Noyan for assistance with the microdiffractometer. The National Synchrotron Light Source at Brookhaven National Laboratory is supported by the US Department of Energy, Division of Materials Sciences and Division of Chemical Sciences.

References:

1. B.S. Meyerson, IBM J. Res. Dev. 44, 391 (2000).
2. B.S. Meyerson, Proc. IEEE 80, 1592 (1992).
3. K. Ismail, S. Rishton, J.O. Chu and B.S. Meyerson, Electron Device Letters 14, 348 (1993).
4. P.M. Mooney, Materials Science and Engineering Reports R17, 105 (1996) and references therein.
5. U. Konig, Mat. Res. Soc. Symp. Proc. 533, 3 (1998).
6. K. Rim, J.L. Hoyt and L.F. Gibbons, IEEE Trans. Electron Devices 47, 1406 (2000).
7. S.J. Koester, R. Hammond, J.O. Chu, P.M. Mooney, J.A. Ott, L Perraud, K.A. Jenkins, C.S. Webster, I. Lagnado and P.R. De La Houssaye, Electron Device Letters, 22, 92 (2000).
8. Z.-H. Cai, W. Rodrigues, P. Ilinski. D. Legnini, B. Lai, W. Yun, E.D. Isaacs, K.E. Lutterodt, J. Grenko, R. Glew, S. Sputz, J. Vandenbuerg, R. People, M.A. Alam, M. Hybertsen, and L.J.P. Ketelsen, Appl. Phys. Lett. 75, 100 (1999).
9. P.M. Mooney. J.L. Jordan-Sweet, I.C. Noyan, S.K. Kaldor, and P.-C. Wang, Appl. Phys. Lett. 74, 726 (1999).
10. P.M. Mooney, J.L. Jordan-Sweet, I.C. Noyan, S.K. Kaldor and P.C. Wang, Physica B 273-274, 608 (1999).
11. "High Resolution X-ray Diffractometry and Topography", D. Keith Bowen and Brian K. Tanner, Taylor and Francis Inc. (Bristol, PA, 1998) pp. 173-4.
12. B.S. Meyerson, Appl. Phys. Lett, 48, 797 (1986); IBM J. Res. Dev. 44, 132 (2000).

13. I.C. Noyan, S.K. Kaldor, P.-C. Wang and J. L. Jordan-Sweet, Rev. Sci. Instrum. 70, 1300 (1999).

14. I.C. Noyan, P.-C. Wang, S.K. Kaldor, J.L. Jordan-Sweet and E.G. Liniger, Rev. Sci. Instrum. 71, 1991 (2000).

15. P.F. Fewster, J. Appl. Cryst. 25, 714 (1992).

16. The extinction depth in Si has been measured to be 3-8 μm (I.C. Noyan, unpublished).

17. S. Yu Shiryaev, F. Jensen, J. Lundsgaard Hansen, J. Wulff Petersen, and A. Nylandsted Larsen, Phys. Rev. Lett.. 78, 503 (1997).

18. P. Sutter and M.G. Lagally, Phys. Rev. Lett. 82, 1490 (1999).

Table I: Characteristics of the SiGe Samples. The uncertainty in the thickness measurement by XTEM is +/-2 nm, in the alloy composition is +/-0.01. (* indicates nominal values, i.e. not measured).

Sample	SiGe Later Thickness (nm)	Alloy Composition, x
A	≃450	0.15
B	43	0.04*
	43	0.09*
	317	0.13
C	43	0.04*
	43	0.09*
	349	0.13
	257	0.17

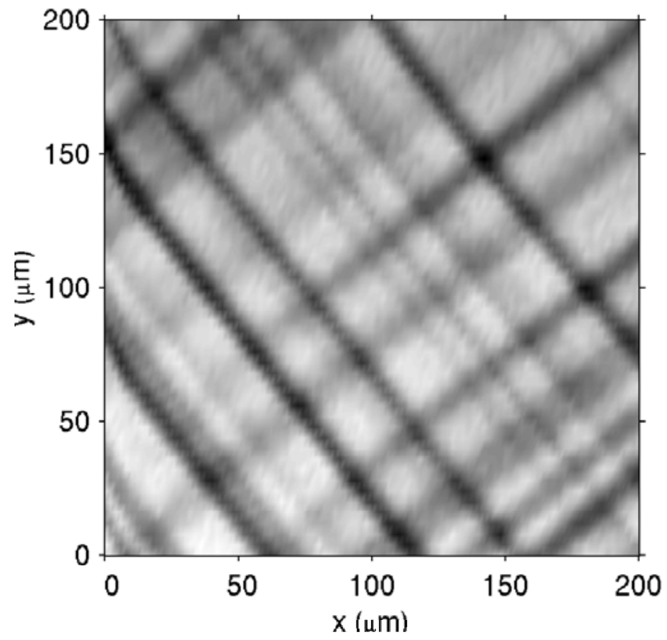

Fig. 1. Scanning x-ray microtopograph taken at the 004 Bragg peak of the $Si_{0.85}Ge_{0.15}$ layer in sample A.

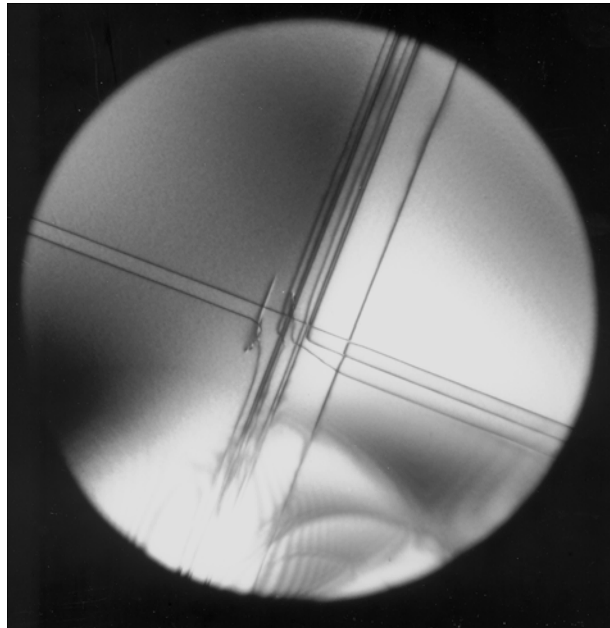

Fig. 2. Planar view TEM image of a dislocated area of sample B showing that the 60o misfit dslocations occur in pileups, not as single isolated dislocations. The diameter of the image is 6.66 mu m.

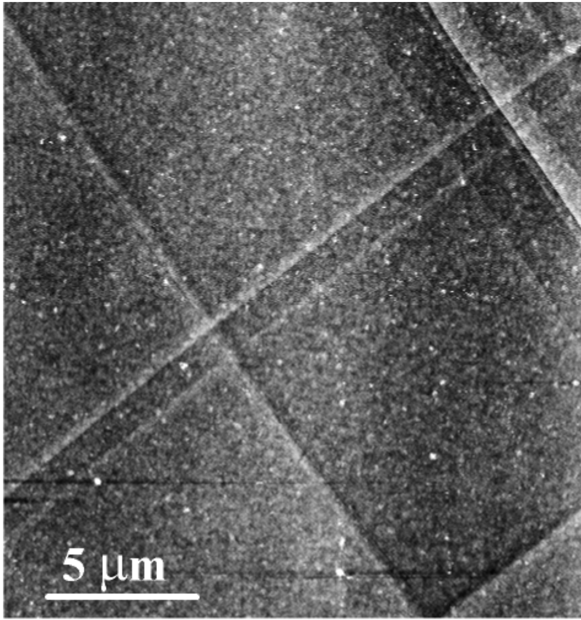

Fig. 3. AFM image of the surface of sample A showing the inhomogeneous distribution of misfit dislocations in these samples.

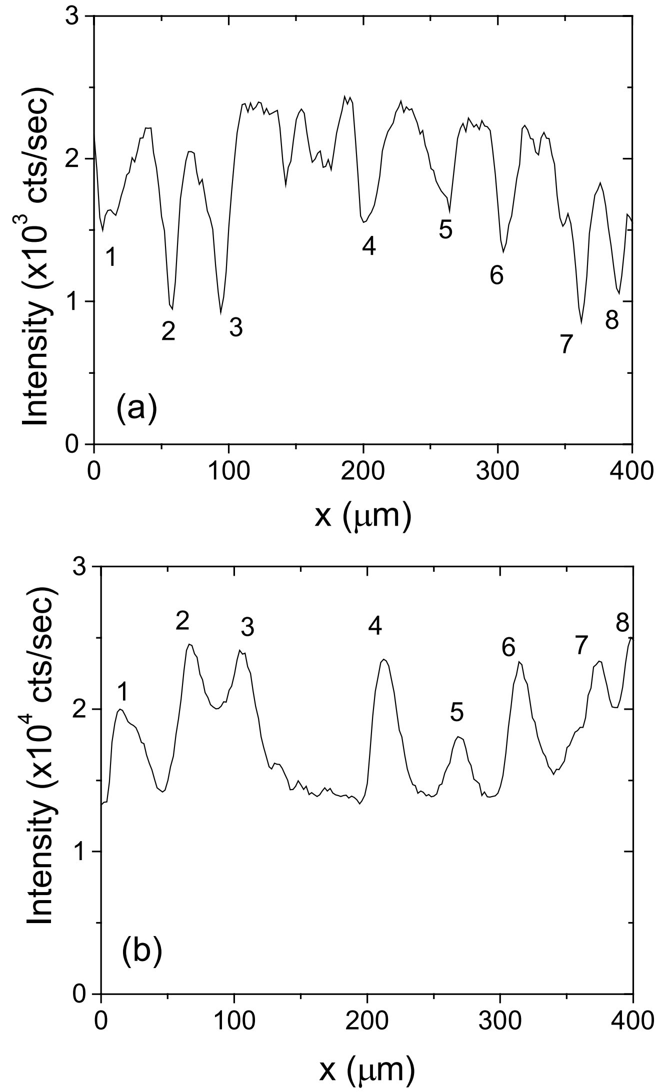

Fig. 4. Microdiffraction line scans taken at the 004 Bragg peak of (a) the Si0.85Ge0.15 layer and (b) the Si substrate of sample A.

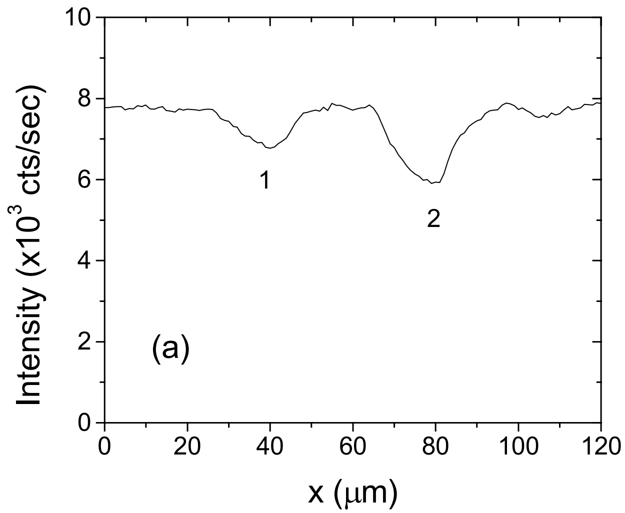

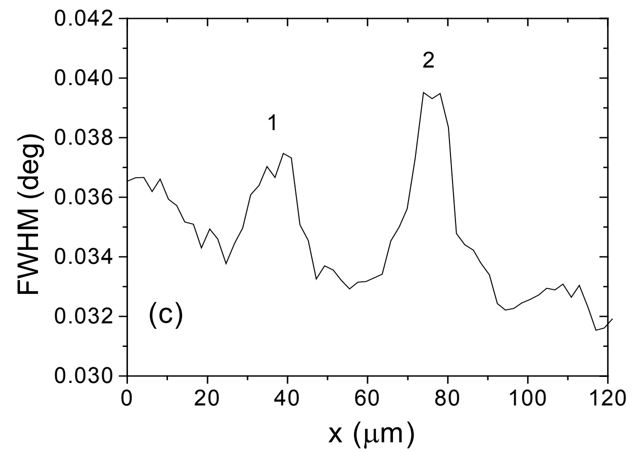

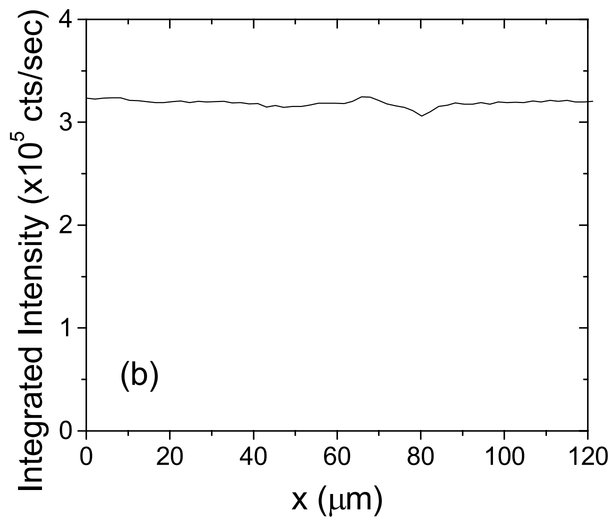

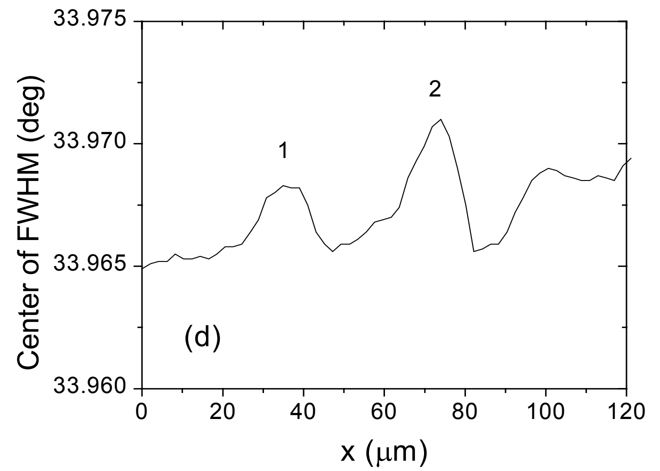

Fig. 5. Line scan taken at the 004 Bragg peak of the Si0.87Ge0.13 layer of sample B (a). The integrated intensity (b) and the FWHM (c) and the center of the FWHM (d) of the rocking curves taken at each x position along the line scan.

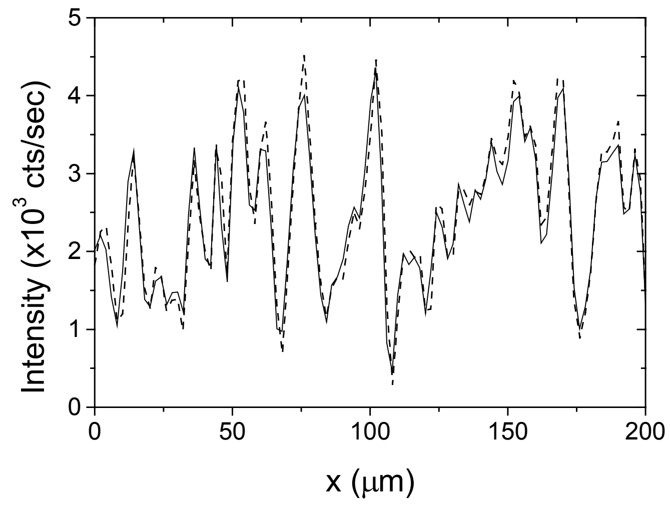

Fig. 6. Microdiffraction line scans taken at the 004 Bragg peaks of (a) the Si0.87Ge0.13 and (b) the Si0.83Ge0.17 layers in sample C. (Note that the error bars are comparable in size to the line width.)